P5.22 MESOSCALE PROCESSES AND IMPACT OF FASTEX CYCLOGENESIS THROUGH MOMENTUM, HEAT, AND WATER BUDGETS (IOPs 11, 12, 16, 17)

A. Protat*, D. Bouniol*, and Y. Lemaître*
Centre d'Etude des Environnements Terrestre et Planétaires (CETP), Vélizy, France

1. INTRODUCTION

In the framework of the GEWEX (Global Energy and Water cycle Experiment) / Cloud System Study (Browning 1994), the major issues of FASTEX (Fronts and Atlantic Storm-Track Experiment, Joly et al. 1997) are to document the internal organization and evolution of mature or developing secondary cyclones, and to establish the impact of these cloud systems on the environment through momentum, heat and water budgets. These issues are the scientific objectives of the present work.

To achieve these objectives, we take advantage of the unprecedented observational dataset collected during FASTEX so as to obtain a description as accurate as possible of the three-dimensional (3-D) fields relevant to this study, namely the three wind components, pressure, temperature, and water contents (vapor, liquid and ice phases, and in both the precipitating and cloudy areas of the cyclones), both at the scale of the cyclones and at the scale of the individual precipitating entities of the cyclones. From these fields, several budgets are computed in order to characterize the impact of cyclogenesis at different scales of motion, which are discussed below.

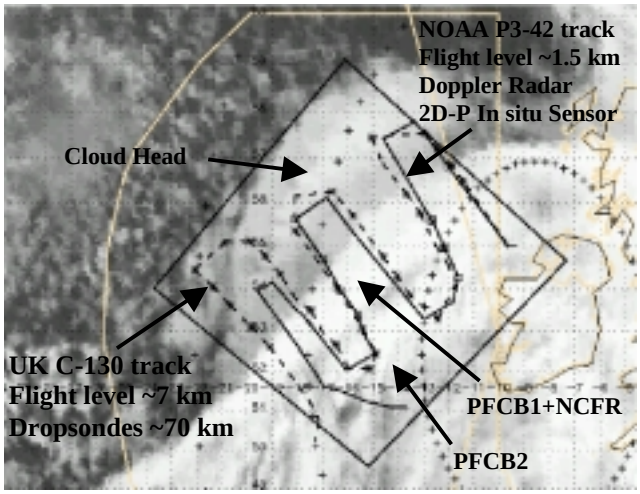

Fig. 1 : Sampling strategy used during FASTEX (mesoscale retrieval box indicated by the rectangle) overlayed to the Meteosat IR image of IOP16 cyclone at 09 UTC. The most important precipitation features are also indicated (cloud head, and two polar front cloud bands PFCB1 (including the narrow cold frontal rainband NCFR) and PFCB2 separated by a strip of reduced cloudiness).

2. DATA AND METHODS

The description of both the mesoscale and convective-scale dynamics of the cyclones is carried out by processing the measurements collected during co-ordinated flight tracks of the two aircraft (NOAA P-3 and NCAR Electra) bearing the airborne Doppler radars and the C-130 aircraft from which dropsondes were launched every 70 km within the cyclones (see Fig. 1). It has been shown recently that the most accurate estimate of the mesoscale 3-D wind field was derived from a combination of the radar and dropsonde data (Bouniol et al. 1999), which has the additional advantage to describe both the precipitating and non-precipitating areas of the cyclone. At the CETP, the 3D wind field at mesoscale and convective-scale is retrieved using the MANDOP analytical method (Scialom and Lemaître 1990), adapted by Montmerle and Lemaître (1998) to include the dropsonde information in the variational process. The 3D fields of pressure, temperature, and water vapor content are retrieved using the analytical method developed by Bouniol et al. (1999). These fields are those used to compute the vertical transport of horizontal momentum, and the heat and moisture budgets.

In order to estimate the water budget of the cyclones, the first step is to retrieve the 3D mesoscale fields of liquid and ice water contents. The method recently developed by Protat et al. (2000) retrieves these fields from a combination of radar and microphysical in-situ 2D-P measurements. The radar is first calibrated in liquid phase by comparing equivalent reflectivities from the radar and reflectivities computed from the particle size distribution using the concept of normalized distribution (Testud et al. 2000). Then, the most representative type of ice is inferred fron a comparison of terminal fall velocity and reflectivities derived from the radar and from an estimate of the same quantities for different types of ice particles. Statistical relationships (precipitation content vs. reflectivity), and (terminal fall velocity vs. reflectivity) are derived from the microphysical in-situ data. These relationships are then used to "translate" the 3D radar reflectivity field into 3D fields of terminal fall velocity and precipitation contents (see Protat et al. 2000).

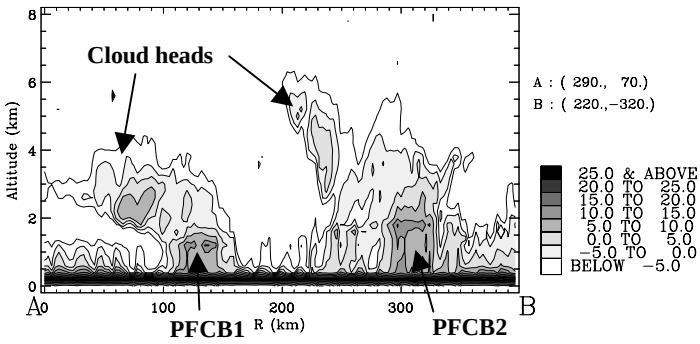

Fig. 2: Illustration of the vertical layering of precipitation within the IOP16 cyclone. Multiple cloud heads are observed.

Finally, in order to perform a full water budget analysis of the cyclones, the 3D field of cloud content must be estimated. Owing to problems of calibration of the 2D-C sensor onboard the P-3, the method of Protat et al. (2000) could not be applied to the 2D-C sensor. Therefore, an indirect method has been developed to access the 3D mesoscale field of cloud content (or saturation deficit if negative, Protat et al. 2001, in preparation). This method relies upon the same principle as Hauser and Amayenc (1986), but adapted in three dimensions and with the ice phase included. This method makes use of the continuity equation for total water substance, with the steady-state assumption in a moving frame of reference:

$$\begin{aligned} \boldsymbol{V}.\nabla q_T - \nabla(K\nabla q_T) = &-(1/\rho)\partial(\rho V_{Tr}\, q_r)/\partial z \\ &-(1/\rho)\partial(\rho V_{Ti}\, q_i)/\partial z \end{aligned} \qquad (1)$$

where q_T ($=q_r+q_i+q_c+q_v$), q_r, q_i, q_c, and q_v are the total water, rainwater, ice, cloud (in liquid or ice phase), and vapor content, respectively, ρ the air density, $\boldsymbol{V}$ the 3D wind vector, K the diffusion coefficient assumed equal to 1500 m^2s^{-1}, V_{Tr} and V_{Ti} the terminal fall speed of hydrometeors in liquid and ice phase, respectively, derived from the method described in Protat et al. (2000). The right-hand side term of (1) is a source term describing sedimentation of water due to the gravitational fall of hydrometeors. The total water content is obtained from (1) using a second-order differentiation scheme and the so-called successive overrelaxation method (described in Hauser and Amayenc 1986). Iterations are repeated until (1) is satisfied with a relative error less than 0.1 %. We retrieve finally the cloud content by subtracting the precipitation and vapor contents to the total water content. Then, the water budget analysis of the cyclones is estimated using the method described in Chong and Hauser (1988).

3. OVERVIEW OF THE SELECTED FASTEX CASES

The purpose of this study is to characterize the multiscale processes involved in cyclogenesis at different stages of development and its impact on the large-scale. In order to broadly cover the life cycle of frontal cyclones, from the weak frontal wave to the explosive cyclogenesis (Shapiro and Keyser 1990), four cases have been selected from the FASTEX database. IOP11 is a deepening primary cyclone with trailing cold and warm fronts. IOP16 is a fast moving rapidly-deepening frontal wave that developed on the trailing cold front of a parent low (see cloud structure at mature stage in Fig. 1). It developed the typical cloud head of a deepening Atlantic storm depression with associated heavy precipitation, pronounced dry intrusion, and strong winds (40 ms^{-1} at 900 hPa). IOP17 is an explosive deepening col wave, characterized by a 40 mb deepening in 24 hours, and a very active cold front that caused some severe weather in UK. IOP12 is the explosive cyclogenesis case, with well-developed cloud head and dry slot features, and an organised line of thunderstorms.

The documentation of precipitation, wind and thermo-dynamics has been completed for the four cases. This documentation evidenced the very complex vertical layering of precipitation and substructures in all cases, including low-level convective entities, midlevel structures, multiple cloud heads, as illustrated in Fig. 2 for IOP16 on a vertical cross-section through the cyclone. This clearly suggests that an inspection of each substructure of the cyclone is mandatory in order to investigate the variety of processes that are probably involved in such an internal organization.

The mesoscale dynamics has been analyzed in detail in light of the conceptual schemes recently proposed in the literature (e.g., Browning and Roberts 1994). The main flows involved in the mesoscale organization of the cyclones have been identified. These flows are in good agreement (e.g., Lemaître et al. 1999, Bouniol et al. 1999) with the proposed conceptual schemes for cyclogenesis at mature stage.

From this documentation, the multiscale processes involved in the mature stage of the IOP16 cyclone have been investigated. Results are presented in detail in this preprint volume (paper **13.7** from Bouniol et al.). It is shown that both low-level/upper-level coupling and mesoscale CSI (Conditional Symmetric Instability) are involved in the intensification of the IOP16 cyclone. The same process study is presently conducted on the three other cases, in order to investigate the potential relationship between the reinforced or inhibited processes and the stage of development reached by the cyclones.

4. MOMENTUM FLUXES

Momentum fluxes are calculated in this section to examine quantitatively the respective contribution of the synoptic-scale, mesoscale, and convective-scale circulations to the vertical transport of horizontal momentum. These momentum fluxes may be written as:

$$\begin{cases} \rho\langle uw\rangle = \rho\langle u\rangle\langle w\rangle + \rho\langle u'w'\rangle \\ \rho\langle vw\rangle = \rho\langle v\rangle\langle w\rangle + \rho\langle v'w'\rangle \end{cases} \qquad (2)$$

where the <> denotes the average over the whole retrieval domain and the prime the deviations from the average. The first term on the right hand side of (2) corresponds to momentum transported at a scale of motion larger than the scale resolved in the wind analysis, while the second term corresponds to momentum transported at the scale of motion resolved by the analysis or smaller.

4.1 On Mesoscale

Fig. 3 shows the along-front and cross-front momentum fluxes derived from the mesoscale wind field retrieved within the IOP16 cyclone. It must be noted that both components of the vertical transport are of equal amount, with peak magnitudes of around 0.4 $kg.m^{-1}s^{-2}$. For both components of the momentum fluxes, the “eddy” fluxes contribute most strongly to the total flux (Fig. 3), except above the 3-km altitude in the along-front transport where the synoptic-scale contribution is significant (Fig. 3a). This indicates that the vertical transport of horizontal momentum is mostly carried out on mesoscale or smaller-

scale where precipitation is present, while the synoptic-scale transport is most important above.

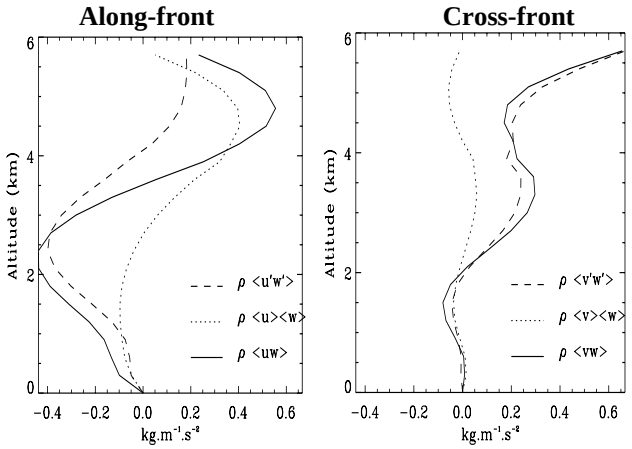

Fig. 3: Along and cross front components of the momentum flux on mesoscale within the IOP16 cyclone.

4.2 At the scale of individual entities of the cyclones

From the convective-scale wind retrievals within selected entities of the cyclones, the contribution of these individual entities to the total momentum flux can be estimated. This is illustrated in what follows for IOP16. As shown in Fig. 1, three main precipitating areas are clearly seen : the cloud head emerging from the polar front cloud band associated with the trailing cold front, and two substructures in the polar front cloud band (denoted PFCB1 and PFCB2 in Fig. 1) separated by a reduced cloudiness strip.

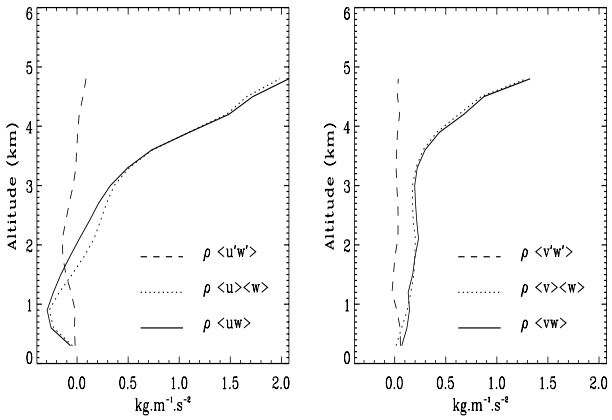

Fig. 4: Along and cross front components of the momentum flux on convective-scale within the cloud head of the IOP16 cyclone.

Fig. 4 shows the momentum fluxes associated with the cloud head. It is clearly seen that vertical transports of horizontal momentum are mostly carried out at a scale of motion larger than the convective-scale (which is the scale resolved by the present wind analysis). This result also applies for the (PFCB1+NCFR) and PFCB2 regions (not shown), except below the 2-km altitude where significant eddy transport is occuring within the NCFR. Since the analysis on mesoscale showed that mesoscale transports were dominant, this means that convective-scale entities are quite passive in terms of momentum flux, which means that the mesoscale is the relevant scale for the momentum transport within the studied frontal cyclones. The only exception to this conclusion is the NCFR that contributes significantly to the total momentum flux. The same results are found within the other IOPs (not shown).

5. HEAT BUDGET OF THE CYCLONES

The "apparent" heat budget (denoted as the Q_1 budget in the literature) characterizes the impact of cyclogenesis in terms of net heating/cooling of the environment. Using the steady-state assumption in a moving frame of reference, this quantity may be defined as

$$Q_1 = \bar{\pi}\,(V - C).\nabla\bar{\theta} \qquad (3)$$

where Π is the nondimensional pressure, θ the potential temperature, $\boldsymbol{C}$ the advection speed vector of the moving frame of reference, and the overbar denotes the average over the whole retrieval domain. This equation may also be rewritten as:

$$Q_1 = -\frac{\bar{\pi}}{\bar{\rho}}\nabla.\overline{(\rho\,\theta' V')} + \bar{\pi}\,\overline{S(\theta)} + D_{Q_1} \qquad (4)$$

where the prime denotes the deviation from the average, D_{Q1} is a subgrid-scale diffusion term (computed in the present case but always negligible), and $S(\theta)$ is a source term reflecting diabatic heating. The first term on the right-hand side of (4) is the eddy heat flux convergence term, reflecting warming/cooling of the environment of the cyclone due to scales resolved by the analysis or smaller. An estimate of the latent heat term is obtained by computing the eddy heat flux convergence term in (4) and subtracting it to Q_1 computed using (3).

Fig. 5 shows the Q_1 budget for the four IOPs discussed in section 3. It is seen from these figures that the general impact of cyclogenesis is to stabilize the atmosphere with a warming throughout the troposphere. For IOP16, this warming, as well as the double-peak vertical structure of the warming, is mostly driven by latent heat release within the cyclones, as shown by the decomposition of the budget into its two components (Fig. 6). However, there are also some signatures of cooling in the low levels in some cases (Fig. 5), corresponding in the case of IOP16 to both rain evaporation and negative eddy flux convergence (Fig. 6). It is also seen that (i) the vertical structure of heating is significantly different from one case to another, which has some implication for the derivation of vertical heating profiles from spaceborne radiometry using a predefined vertical structure, and (ii) the most intense secondary cyclones result in strongest warming (peaks are around 30-40 K/day). More comparisons will be presented at the conference regarding the differences between the four cyclones.

As for the momentum fluxes, the heat budget of the individual precipitating entities of the cyclones have been estimated from the convective-scale retrievals. Within IOP16, it is found that all regions contribute significantly to the total heat budget but at different heights (which explains the double-peak structure), and that diabatic processes are dominant in the cloud head and PFCB2

regions, while both diabatic processes and eddy flux convergence contribute to the total heating within the (PFCB1+NCFR) region (not shown).

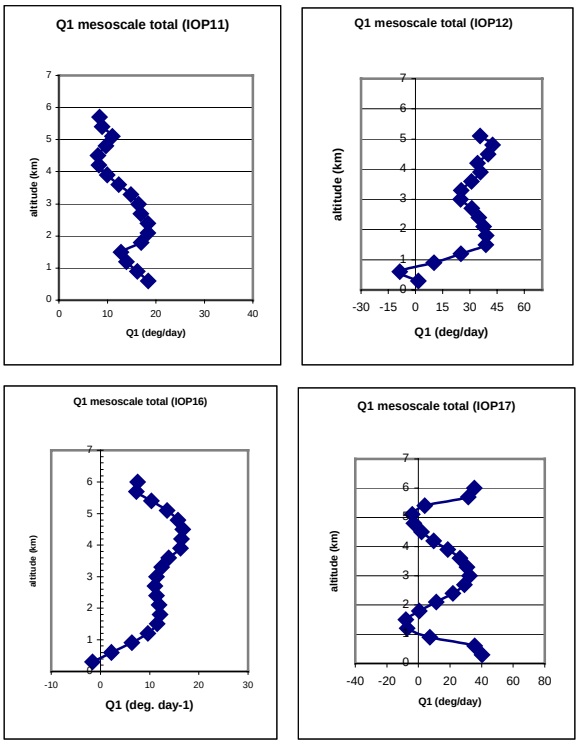

Fig. 5: Vertical profile of the heat source on mesoscale for IOPs 11, 12, 16, and 17.

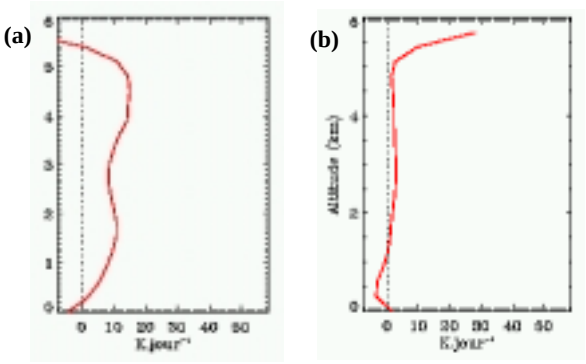

Fig. 6: Components of the IOP16 heat budget: (a) the latent heat release term, and (b) the eddy heat flux convergence term.

6. MICROPHYSICAL PROCESSES

As discussed in section 2, a method for retrieval of the 3D field of cloud content has been recently developed at CETP. Fig. 7b shows the retrieved cloud content (or saturation deficit if negative) in a vertical cross-section through the cloud head of IOP16. It is observed that the maximum cloud content is retrieved at the location of the cloud head (Figs. 7ab), with magnitudes (1 to 1.2 g.kg-1) comparable to observations within narrow cold frontal rainbands (Marécal et al. 1993), with a cloud base located around the 1-km altitude in this region. This cloud content is presently being validated before conducting the water budget analysis of the FASTEX cyclones.

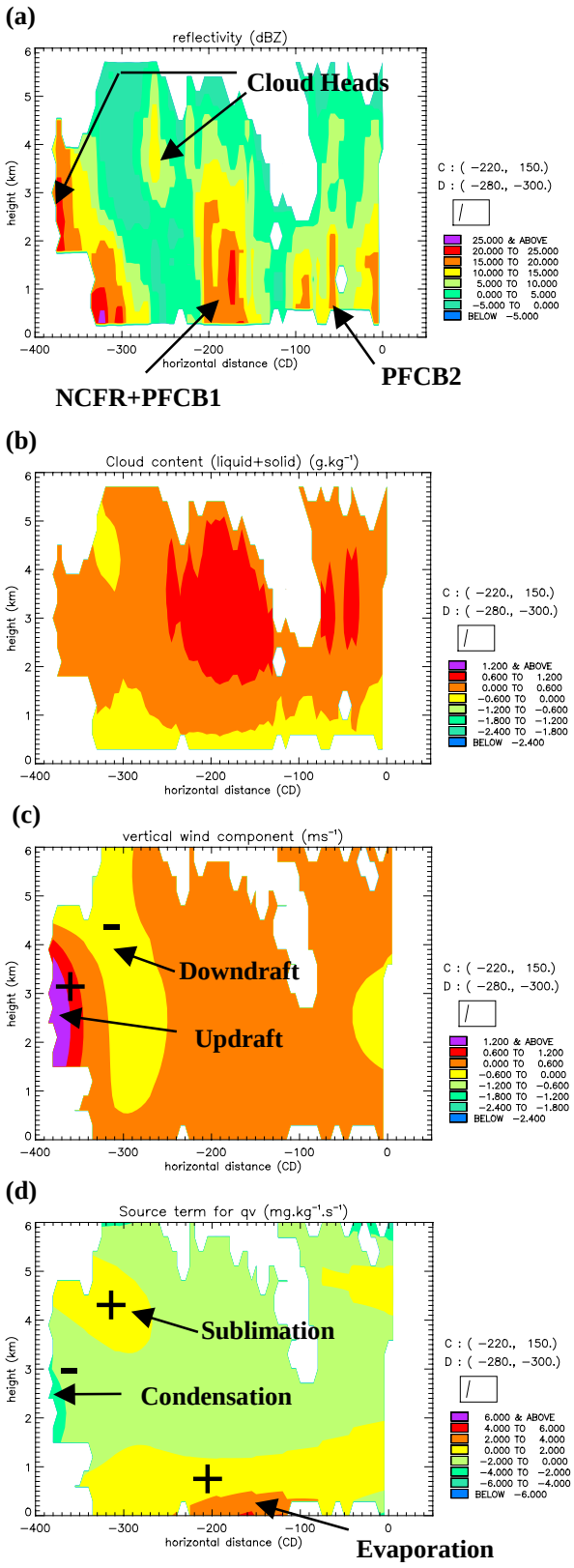

Fig. 7: Vertical cross-section through the IOP16 cloud head. (a) reflectivity, (b) retrieved cloud content or saturation deficit, (c) vertical wind component, and (d) source term of the continuity equation for water vapor.

It is important to note here that the retrieval of the 3D structure of all the water contents offers a unique opportunity to access the microphysical processes involved in cyclogenesis at mature stage. These microphysical processes can be investigated from the source terms of the continuity equations for each water substance (see for instance Marécal et al. 1993). This is illustrated in Fig. 7d, showing the source term of the continuity equation for water vapor. Fig. 7d shows a positive area (source of water vapor in an ice region) located downslope of the cloud head (see Fig. 7a), associated with the main downdraft (Fig. 7c). This configuration corresponds to sublimation of ice in a descending flow, which has been recently proposed from modelling studies (Clough and Franks 1991; Clough et al. 2000) as a crucial mechanism for supporting moist adiabatic descent within cloud features typical of frontal cyclones. This preliminary result (to be validated, as discussed just above) provides thus an observational support to the so-called Clough-Franks mechanism of sublimation-enhanced descent.

6. PERSPECTIVES

Our first short-term perspective is obviously to validate the retrieved 3D field of cloud content by using all relevant sources of data, including the numerous dropsondes launched within the precipitation areas. Then, a full water budget analysis of the IOP16 frontal cyclone will be conducted, following the methodology proposed by Chong and Hauser (1988). This water budget analysis will be discussed in detail at the conference. Then, the three other selected frontal cyclones will be interpreted in terms of multiscale processes, momentum, heat, and water budgets. Special emphasis will be put on the differences observed between these four cyclones, in order to investigate the potential relationship between the development stage reached by the cyclones, the involved processes, and their impact on the large-scale environment.

Acknowledgments

The present work is supported by the Programme Atmosphère et Océan à Moyenne échelle of the Institut National des Sciences de l'Univers under contract 97/01, and by the European Commission under contract ENV4-CT96-0322. We are indebted to our UKMO colleagues who provided us with the C-130 validated dropsonde data, and to R. Black (HRD, Miami, USA) who processed and provided us with the P3 2D-P sensor data.

References

Bouniol, D., A. Protat, and Y. Lemaître, 1999: Mesoscale dynamics of a deepening secondary cyclone (FASTEX IOP16): Three-dimensional structure retrieved from dropsonde data. *Quart. J. Roy. Meteor. Soc.*, **125**, 3535-3562.

Browning, K. A., 1994: GEWEX Cloud System Study (GCSS): science plan. IGPO Publication Series No 11. Reading, UK.

Browning, K. A., and N. M. Roberts, 1994 : Structure of a frontal cyclone. *Quart. J. Roy. Meteor. Soc.*, **120**, 1535-1557.

Chong, M. and D. Hauser, 1988: A tropical squall line observed during the COPT81 experiment in West Africa. Part II: Water budget. *Mon. Wea. Rev*., **117**, 728-744.

Clough, S.A., and R.A. Franks, 1991: The evaporation of frontal and other stratiform precipitation. *Quart. J. Roy. Meteor. Soc.*, **117**, 1057-1080.

Clough, S.A., H.W. Lean, N. M. Roberts, and R.M. Forbes, 2000: Dynamical effects of ice sublimation in a frontal wave. *Quart. J. Roy. Meteor. Soc.*, **126**, 1-36.

Hauser, D. and P. Amayenc, 1989: Retrieval of cloud water and water vapor contents from radar data in a tropical squall line. *J. Atmos. Sci.*, **43**, 823-827.

Joly, A., and Co-authors, 1997: The Fronts and Atlantic Storm-Track Experiment (FASTEX): scientific objectives and experimental design. *Bull. Am. Meteor. Soc.*, **78**, (9), 1917-1940.

Lemaître, Y., A. Protat, and D. Bouniol, 1999: Pacific and Atlantic "bomb-like" deepenings in mature phase: A comparative study. *Quart. J. Roy. Meteor. Soc.*, **125**, 3513-3534.

Marécal, V., D. Hauser, and F. Roux, 1993: The NCFR observed on 12-13 January 1988 during the MFDP/FRONTS87 Experiment. Part II: Microphysics. *J. Atmos. Sci.*, **50**, 975-998.

Montmerle, T, and Y. Lemaître, 1998: 3D variational data analysis to retrieve thermodynamical and dynamical fields from various nested wind measurements. *J. Atmos. Oceanic Technol.*, **15**, 360-379.

Protat, A., Y. Lemaître, D. Bouniol, and R. A. Black, 2000: Microphysical observations during FASTEX from airborne doppler radar and in-situ measurements. Phys. Chem. Earth (B), **25**, 1097-1102.

Scialom, G., and Y. Lemaître, 1990: A new analysis for the retrieval of the three-dimensional wind field from multiple Doppler radars, *J. Atmos. Oceanic Technol.*, **7**, 640-665.

Shapiro, M. A., and D. Keyser, 1990: Fronts, jet-streams and Tropopause. In Extratropical cyclones: the Erik Palmen Memorial Volume, C.W Newton and E.O.Holopainen, Eds. American Meteorological Society, 167-191.

Testud, J., S. Oury, R. Black, P. Amayenc, and X.-K. Dou, 2000 : The concept of normalized distribution to describe raindrop spectra : a tool for cloud physics and cloud remote sensing. *J. Appl. Meteor.*, in press.